

# Ankyrin-G Inhibits Endocytosis of Cadherin Dimers\*

Received for publication, February 25, 2015, and in revised form, November 12, 2015. Published, JBC Papers in Press, November 16, 2015, DOI 10.1074/jbc.M115.648386

Chantel M. Cadwell<sup>†1</sup>, Paul M. Jenkins<sup>§2</sup>, Vann Bennett<sup>§</sup>, and Andrew P. Kowalczyk<sup>¶||\*\*3</sup>

From the <sup>†</sup>Biochemistry, Cell, and Developmental Biology Graduate Program, <sup>¶</sup>Department of Cell Biology, <sup>||</sup>Department of Dermatology, and <sup>\*\*</sup>Winship Cancer Institute, Emory University School of Medicine, Atlanta, Georgia 30322 and the <sup>§</sup>Howard Hughes Medical Institute, Department of Biochemistry, Cell Biology, and Neurobiology, Duke University Medical Center, Durham, North Carolina 27710

Dynamic regulation of endothelial cell adhesion is central to vascular development and maintenance. Furthermore, altered endothelial adhesion is implicated in numerous diseases. Therefore, normal vascular patterning and maintenance require tight regulation of endothelial cell adhesion dynamics. However, the mechanisms that control junctional plasticity are not fully understood. Vascular endothelial cadherin (VE-cadherin) is an adhesive protein found in adherens junctions of endothelial cells. VE-cadherin mediates adhesion through *trans* interactions formed by its extracellular domain. *Trans* binding is followed by *cis* interactions that laterally cluster the cadherin in junctions. VE-cadherin is linked to the actin cytoskeleton through cytoplasmic interactions with  $\beta$ - and  $\alpha$ -catenin, which serve to increase adhesive strength. Furthermore, p120-catenin binds to the cytoplasmic tail of cadherin and stabilizes it at the plasma membrane. Here we report that induced *cis* dimerization of VE-cadherin inhibits endocytosis independent of both p120 binding and *trans* interactions. However, we find that ankyrin-G, a protein that links membrane proteins to the spectrin-actin cytoskeleton, associates with VE-cadherin and inhibits its endocytosis. Ankyrin-G inhibits VE-cadherin endocytosis independent of p120 binding. We propose a model in which ankyrin-G associates with and inhibits the endocytosis of VE-cadherin *cis* dimers. Our findings support a novel mechanism for regulation of VE-cadherin endocytosis through ankyrin association with cadherin engaged in lateral interactions.

Dynamic regulation of endothelial cell adhesion is central to normal vascular development and maintenance. Furthermore, altered endothelial adhesion is associated with aberrant angiogenesis and contributes to numerous diseases through increased inflammation (1–3). Therefore, normal vascular patterning and maintenance requires tight regulation of endothelial cell adhesion dynamics. However, the mechanisms that control junctional plasticity are not fully understood.

\* This work was supported by National Institutes of Health Grants RO1AR050501 and RO1AR048266 (to A. P.K.). The authors declare that they have no conflicts of interest with the contents of this article. The content is solely the responsibility of the authors and does not necessarily represent the official views of the National Institutes of Health.

<sup>1</sup> Supported by a fellowship from the American Heart Association.

<sup>2</sup> Present address: Departments of Pharmacology and Psychiatry, University of Michigan Medical School, Ann Arbor, MI 48109.

<sup>3</sup> To whom correspondence should be addressed: Depts. of Cell Biology and Dermatology, Winship Cancer Institute, Emory University School of Medicine, Atlanta, GA. Tel.: 404-727-8517; Fax: 404-727-6256; E-mail: akowalc@emory.edu.

Adherens junctions are cadherin-based intercellular structures that mediate adhesion and mechanically link adjacent cells (4). Vascular endothelial cadherin (VE-cadherin)<sup>4</sup> is the major adhesive protein in the adherens junctions of the endothelium. Modulation of VE-cadherin levels at the plasma membrane contributes to the dynamic regulation of adhesion (5). Like other classical cadherins, VE-cadherin binds to members of the armadillo family of proteins, called catenins, through its cytoplasmic tail. p120-catenin (p120) stabilizes VE-cadherin at the cell surface through binding to the juxtamembrane domain and masking an endocytic motif (6, 7). When p120 is not bound, the cadherin undergoes rapid clathrin-dependent endocytosis and degradation (8–10).  $\beta$ -Catenin binds to the catenin-binding domain of the cadherin cytoplasmic tail. Through interactions between  $\beta$ - and  $\alpha$ -catenin, the cadherin is linked to the actin cytoskeleton, which increases the adhesive strength of the junction (11–15).

VE-cadherin mediates adhesion through its extracellular domain by the formation of calcium-dependent homophilic *trans* interactions. *Trans* interactions occur between two cadherins on neighboring cells and are believed to be the initial recognition events in the formation of adherens junctions (16, 17). Adhesion occurs through a reciprocal process in which a conserved tryptophan (Trp-2) is inserted into a hydrophobic pocket of a cadherin on a neighboring cell (18, 19). *Cis* interactions, interactions between two cadherins on the surface of the same cell, laterally cluster VE-cadherin (16, 20). Together, *cis* and *trans* interactions coalesce the cadherin into cell junctions.

Neighboring endothelial cells are coupled mechanically through linkage of VE-cadherin to the cytoskeleton. The actin cytoskeleton of endothelial cells is composed of three separate but interrelated structures: the membrane skeleton, the cortical actin ring, and actomyosin-based stress fibers (21). The membrane skeleton, often referred to as the spectrin-actin cytoskeleton, is immediately adjacent to the plasma membrane, and it is responsible for membrane architecture (21). It primarily consists of spectrin and spectrin binding partners, including ankyrin-G. Ankyrin-G binds to membrane proteins and, through associations with spectrin, links them to the cytoskeleton. Ankyrin-G binding partners include cell adhesion molecules such as L1 cell adhesion molecule and E- and N-cadherin (22).

<sup>4</sup> The abbreviations used are: VE-cadherin, vascular endothelial cadherin; FKBP, FK506 binding protein; HUVEC, human umbilical vein endothelial cell.

## Ankyrin-G Inhibits Endocytosis of Cadherin Dimers

Among most classical cadherins, including E-cadherin, the ankyrin-G-binding site is highly conserved and spans a region of the cytoplasmic tail that includes the juxtamembrane domain (23). In polarized epithelial cells, ankyrin-G binds to E-cadherin and retains it at the lateral wall (24). In Madin-Darby canine kidney cells, E-cadherin at the apical membrane undergoes clathrin-mediated endocytosis. In contrast, E-cadherin at the lateral membrane is bound by ankyrin-G and stabilized at the surface. In this way, ankyrin-G, in cooperation with clathrin, contributes to the polarized epithelial phenotype.

To better understand the mechanisms that regulate endothelial cell adhesion, we studied the relationship between homophilic VE-cadherin interactions involved in adherens junction formation and cadherin endocytosis. Our data demonstrate that *cis* dimerization inhibits VE-cadherin endocytosis independent of *trans* interactions. Inhibition of endocytosis through *cis* dimerization is not dependent on p120 binding to the cadherin. However, we found that ankyrin-G associates with cadherin *cis* dimers and inhibits endocytosis of VE-cadherin. Our findings support a novel mechanism for regulation of VE-cadherin endocytosis through ankyrin-G association with cadherin engaged in lateral interactions.

### Experimental Procedures

**Cell Culture**—The African green monkey kidney fibroblast-like (COS-7, ATCC) and HEK QBI-293A cell lines (MP Bio-medicals) were cultured as described previously (6). Primary mouse endothelial cells were cultured as described previously (25). Human dermal microvascular endothelial cells were cultured in endothelial growth medium 2 microvascular (Lonza). Human umbilical vein endothelial cells were cultured in M199 (Mediatech, Inc.) supplemented with 20% FBS and 1% penicillin/streptomycin on gelatin-coated plates.

**Virus Production**—To generate an adenoviral expression system for protein expression in mammalian cells, the gene of interest was cloned into the gateway pAd/CMV/V5-DEST vector (Invitrogen). The vector was linearized using PacI and transfected into HEK QBI293 cells to produce virus. After several rounds of infection, cells were lysed, and virus was harvested.

**Generation of VE-cadherin cDNA Constructs**—FKBP fusion proteins were generated using the ARGENT regulated homodimerization kit (ARAID Pharmaceuticals Inc., Cambridge, MA) by subcloning a single FKBP domain followed by a HA tag in-frame with N terminus of the cadherin. VE-cadherin- $\Delta$ catenin-binding domain (CBD)-FKBP was generated by the addition of a single FKBP domain with a HA tag to the end of the juxtamembrane domain of the VE-cadherin tail. The Trp-2 mutation was introduced using site-directed mutagenesis with the following primers: 5'-CGCCAAAAGAGAGATGCAATTTGGAACAGATG-3' and 5'-CATCTGGTTCCAAATTGCATCTCTCTTTTGGCG-3'. The GGG  $\rightarrow$  AAA mutation was introduced using primers described previously (6).

**Dimerization of VE-cadherin-FKBP Fusion Proteins**—To induce dimerization, cells were incubated with 1  $\mu$ l of 100  $\mu$ M AP20187 (ARGENT, ARAID Pharmaceuticals, Inc.) or 1  $\mu$ l of ethanol (vehicle control) in 1 ml of DMEM + 10% FBS for 2 h at

37 °C. Cells were washed three times with DMEM before being used for downstream applications.

**shRNA Transfection in HUVECs**—HUVECs cultured on gelatin coverslips were transfected using Targefect-HUVEC (Targetingsystem, El Cajon, CA) according to the protocol provided by the supplier with a pLentilo3.7 plasmid encoding shRNA against ankyrin-G (5'-GGATTAAGCAGGAAAGCAACC-3') or luciferase (5'-CGTTACCGCGGAATACTTCGA-3') under the U6 promoter and mCherry under the  $\beta$ -actin promoter. For rescue experiments, endothelial cells were co-transfected with ankyrin-G shRNA and HA-tagged, 190-kD ankyrin-G. HA-tagged ankyrin-G was generated using the coding sequence of the 190-kDa isoform of ankyrin-G described previously (26) and inserted into the EcoRI and PmeI sites of the pEGFP-N3 vector in which the enhanced GFP had been replaced by a 3 $\times$  HA tag using standard molecular biology techniques. After 48 h, immunofluorescence or Western blot analysis was performed. For immunofluorescence, mCherry was used to detect transfected cells.

**Immunoprecipitation and Western Blot Analysis**—For immunoprecipitation experiments, COS-7 cells were pretreated with 1 mM dithiobis(succinimidyl propionate) (Thermo Scientific, Pierce) for 2 h at 4 °C to cross-link proteins. To quench the cross-linking reaction, cells were incubated with 25 mM Tris (pH 7.5) at 4 °C for 15 min. Cells were harvested in 0.5% Triton X-100 (Roche) containing protease inhibitor mixtures (Complete mini tablets, EDTA-free, Roche), 150 mM sodium chloride, 10 mM Hepes, 1 mM EGTA, and 0.1 mM magnesium chloride. After a 30-min incubation at 4 °C, cell lysates were centrifuged at 16,100  $\times$  g for 10 min and then incubated with 2  $\mu$ g of anti-HA (Bethyl Laboratories, Inc.) conjugated to ferromagnetic beads (Dynabeads, Life Technologies) for 2 h at 4 °C with full rotation. The beads were then washed with 0.1% Triton X-100 and eluted into Laemmli sample buffer (Bio-Rad) with 5%  $\beta$ -mercaptoethanol.

For Western blot experiments, cells were harvested directly into sample buffer. Samples were heated at 95 °C for 5 min, separated by SDS-PAGE, and analyzed by immunoblotting on nitrocellulose membranes (Whatman). Primary antibodies were as follows: rabbit anti-ankyrin-G C-terminal domain, anti-p120 (rabbit polyclonal Ser-19, Santa Cruz Biotechnology, Inc.), cadherin-5 (BD Transduction Laboratories), monoclonal anti-vimentin clone V9 (Sigma-Aldrich), and rabbit anti- $\beta$ -tubulin (Santa Cruz Biotechnology). For protein detection, horseradish peroxidase-conjugated secondary antibodies (Bio-Rad) and a luminol-based detection system (ECL, GE Healthcare) were used, followed by exposure to autoradiography film (Denver Scientific).

**Internalization and Localization Assays**—Cells were infected with VE-cadherin mutants using an adenoviral expression system, or cells were transfected using Lipofectamine 2000 (Invitrogen) according to the protocol provided by the supplier. Internalization assays were performed as described previously (7, 9). Briefly, cells cultured on glass coverslips were incubated with an antibody against the VE-cadherin extracellular domain in medium for 30 min at 4 °C. Cells were washed three times with cold PBS to remove unbound antibody. To allow internalization, cells were incubated in prewarmed medium for 30 min

for VE-cadherin or 5 min for the transferrin receptor at 37 °C. Cells were returned to cold medium. A low-pH buffer (PBS with 100 mM glycine, 20 mM magnesium acetate, and 50 mM potassium chloride (pH 2.2)) was used to remove any remaining antibody from the cell surface. Cells were then fixed and permeabilized by incubation in 4% paraformaldehyde for 10 min, followed by 0.1% Triton X-100 for 8 min at room temperature. Rabbit anti-HA antibody (Bethyl Laboratories, Inc.) was used to determine the total cadherin pool. Secondary antibodies conjugated to fluorescent dyes (Alexa Fluor 488, 555, or 647 nm; Life Technologies) were used to visualize antibody binding. For each cell, internalization was quantified as the ratio of fluorescence signals corresponding to the internalized and total cadherin pools. For localization assays, endothelial cells or cells co-transfected with VE-cadherin and GFP-tagged or HA-tagged 190-kD ankyrin-G were fixed and processed for immunofluorescence. Antibodies used included chicken c-myc antibody (Bethyl Laboratories, Inc.); transferrin from human serum and Alexa Fluor 555 conjugate (Molecular Probes); anti-VE-cadherin antibody and clone BV6 (Millipore); rabbit anti-ankyrin-G and anti-p120-catenin (rabbit polyclonal Ser-19, Santa Cruz Biotechnology, Inc.), and anti- $\beta$ -catenin (rabbit, Sigma-Aldrich). Colocalization was quantified in individual cells using Pearson's correlation coefficient for VE-cadherin and ankyrin-G pixel intensities.

Microscopy was performed using an epifluorescence microscope (DMRXA2, Leica) equipped with  $\times 63$  and  $\times 100$  oil immersion objectives with apochromatic aberration and flat field corrections, narrow band pass filters, and a digital camera (ORCA-ER C4742-80, Hamamatsu Photonics). Images were captured using Simple PCI software (Hamamatsu Photonics).

**Image Analysis and Statistics**—ImageJ software was used for all image analyses (27). Custom ImageJ plugins were used to automate data quantification. R was used to compute statistics.

## Results

**Induced Dimerization of VE-cadherin Inhibits Endocytosis Independent of Adhesion**—To determine how adhesion affects VE-cadherin internalization, we introduced a point mutation to a conserved tryptophan (Trp-2) in the extracellular domain of VE-cadherin (VE-cadherin-Trp-2). The Trp-2 mutation has been shown previously to disrupt VE-cadherin homophilic adhesion (28). Using a fluorescence-based internalization assay that allowed us to specifically observe the internalized pool of the cadherin, we found that VE-cadherin-Trp-2 endocytosis was increased significantly over wild-type VE-cadherin (Fig. 1, A and B). Additionally, instead of junctional clustering, we observed that the Trp-2 mutation resulted in a diffuse localization of the cadherin on the plasma membrane (Fig. 1A). Expression levels between wild-type VE-cadherin and VE-cadherin-Trp-2 were relatively similar by Western blot (Fig. 1C).

*Trans* interactions are thought to occur before *cis* interactions (16, 17). Therefore, the increase in VE-cadherin internalization may be the result of either the loss of adhesive *trans* interactions or lateral *cis* dimerization. To distinguish between these two possibilities, we used the FKB506 binding protein homodimerizing system to model cadherin *cis* clustering. AP20187 is a cell-permeant molecule that can induce the

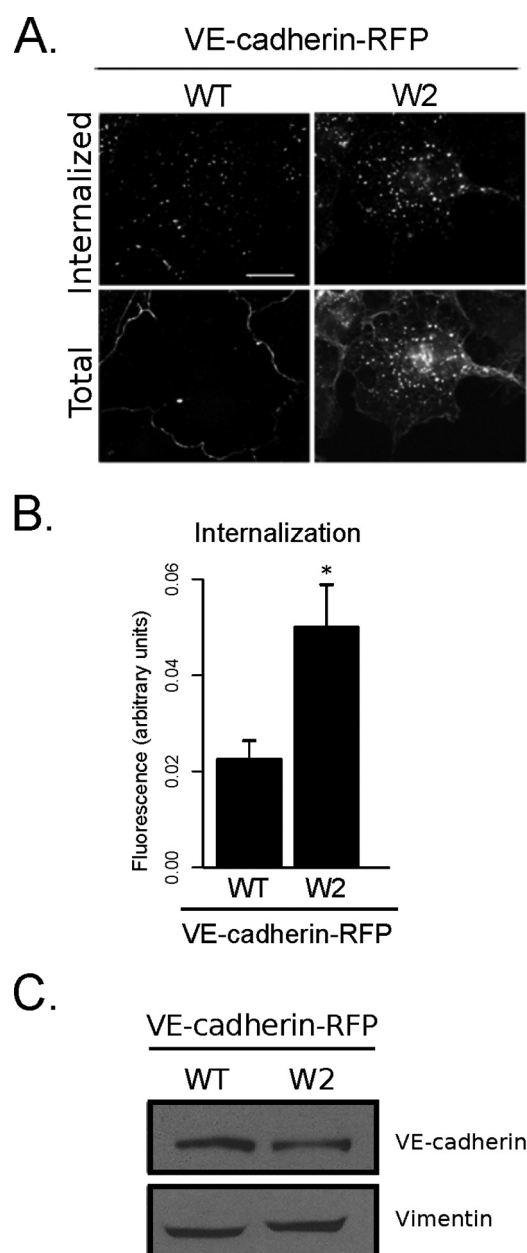


**FIGURE 1. Mutation of conserved tryptophan (Trp-2) increases VE-cadherin internalization.** A, fluorescence-based internalization assay of wild-type (left panels) or non-adhesive (Trp-2) VE-cadherin (right panels) proteins expressed in COS-7 cells. The VE-cadherin-internalized pool (top panels) was identified using anti-VE-cadherin antibody. After a 30-min internalization period, a low-pH wash was used to remove the remaining surface antibody. The total pool (bottom panels) was determined by fluorescence of the red fluorescent protein (RFP) tag fused to the C terminus of the cadherin. Scale bar = 20  $\mu$ m. B, quantification of internalization, determined by normalizing the internalized pool to the total pool. Error bars represent mean  $\pm$  S.E.  $n > 20$  cells/group. \*,  $p < 0.05$ . C, Western blot for expression levels of cadherin (top panel) or vimentin as a loading control (bottom panel) in COS-7 cells.

dimerization of proteins containing FKB506 protein repeats. We fused a FKB506 binding protein (FKBP) repeat to the intracellular C terminus of the VE-cadherin tail (VE-cadherin-FKBP) (Fig. 2A). FK binding proteins have been used previously to study endocytosis of other membrane proteins and are not known to disrupt cadherin localization (29–33). We verified expression by Western blot analysis and junctional localization of VE-cadherin-FKBP using immunofluorescence microscopy

## Ankyrin-G Inhibits Endocytosis of Cadherin Dimers

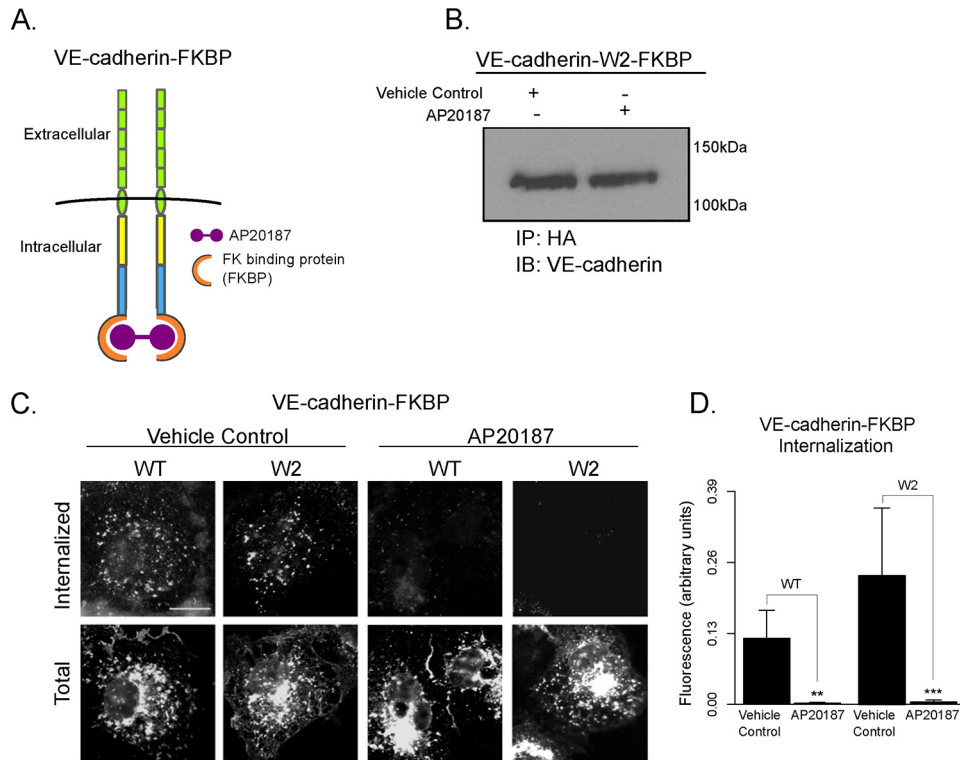


**FIGURE 2. Induced dimerization of VE-cadherin inhibits its endocytosis independent of adhesion.** *A*, schematic of the VE-cadherin-FKBP fusion protein. FKBP is dimerized by the cell-permeant bivalent molecule AP20187. *B*, isolation of HA-tagged VE-cadherin-Trp-2-FKBP by immunoprecipitation (IP) of lysate from COS-7 cells expressing either wild-type VE-cadherin or VE-cadherin-Trp-2 after treatment with vehicle control or AP20187 followed by Western blot for VE-cadherin. *IB*, immunoblot. *C*, internalization assay of cells expressing either wild-type VE-cadherin or VE-cadherin-Trp-2 after treatment with vehicle control or AP20187. *Scale bar* = 20  $\mu$ m. *D*, quantification of the internalization assay. *Error bars* represent mean  $\pm$  S.E. *n* = 10–25 cells/group. \*\*, *p* < 0.01 compared with vehicle control-treated WT. \*\*\*, *p* < 0.001 compared with vehicle control-treated Trp-2.

via an HA tag fused to the C terminus of the protein (Fig. 2, *B* and *C*, bottom left panels). We then introduced the Trp-2 mutation to VE-cadherin-FKBP to generate a VE-cadherin mutant that is not adhesive but that can be induced to form a dimer (VE-cadherin-W2-FKBP). Using an internalization assay, we observed that induced dimerization of the both VE-cadherin-FKBP and VE-cadherin-W2-FKBP cadherin fusion proteins resulted in decreased internalization (Fig. 2, *C* and *D*). Therefore, *cis* interactions independent of *trans* interactions strongly inhibit VE-cadherin endocytosis.

**p120-catenin Binding Is Not Required for Inhibited Endocytosis of VE-cadherin Dimers**—Because p120-catenin is a known regulator of cadherin stability at the cell surface, we hypothesized that p120 binding stabilizes VE-cadherin dimers. To determine the role of p120 in VE-cadherin dimer endocytosis, we first compared the amount of p120 bound to dimerized cadherin to non-dimerized cadherin by immunoprecipitation. However, we found no observable difference in the amount of p120 that co-immunoprecipitated with VE-cadherin in cells treated with AP20187 compared with VE-cadherin in cells treated with vehicle control (Fig. 3A).

To further investigate the role of p120 binding in endocytosis of VE-cadherin dimers, we mutated three glycine residues to alanines in the p120 core-binding domain in the VE-cadherin-FKBP fusion protein (VE-cadherin-GGG-FKBP). Mutation of these three glycine residues (649–651) has been described previously to disrupt p120 binding and to increase endocytosis of the cadherin compared with the wild type (6). As expected,

dimerization of VE-cadherin-GGG-FKBP did not result in p120 binding (Fig. 3B). However, using an internalization assay, we found that inducing dimerization of VE-cadherin-GGG-FKBP inhibited endocytosis (Fig. 3, *C* and *D*). Additionally, we found that dimerization of a VE-cadherin mutant lacking the catenin-binding domain (VE-cadherin- $\Delta$ CBD-FKBP) also inhibited endocytosis (Fig. 3, *E* and *F*). Together, these results indicate that VE-cadherin dimers are resistant to endocytosis in the absence of either p120 or  $\beta$ -catenin binding.

**VE-cadherin Colocalizes with and Co-immunoprecipitates with Ankyrin-G**—Because p120 binding is not required to inhibit endocytosis of dimerized VE-cadherin, we reasoned that another protein might be involved in stabilizing the cadherin at the plasma membrane. One such candidate protein is ankyrin-G, which binds to E-cadherin at conserved sites in the cadherin tail (Fig. 4A) and retains the cadherin at the lateral membrane in polarized epithelial cells (24). The canonical 190/210-kD ankyrin-G isoforms are expressed in endothelial cells, including HUVECs, although expression of both isoforms was not detected in any endothelial cells examined (Fig. 4B). Interestingly, the ankyrin-G-binding motif identified in the cytoplasmic tail of E-cadherin is not fully conserved in VE-cadherin (Fig. 4A) (24). However, by immunofluorescence microscopy, we observed that, in HUVECs, endogenous ankyrin-G localized to various regions of the cells, including cell-cell junctions, where the protein colocalized with VE-cadherin (Fig. 4C). Additionally, ankyrin-G colocalized with wild-type VE-cadherin when co-expressed in COS-7 cells (Fig. 4, *D* and *E*). Inter-

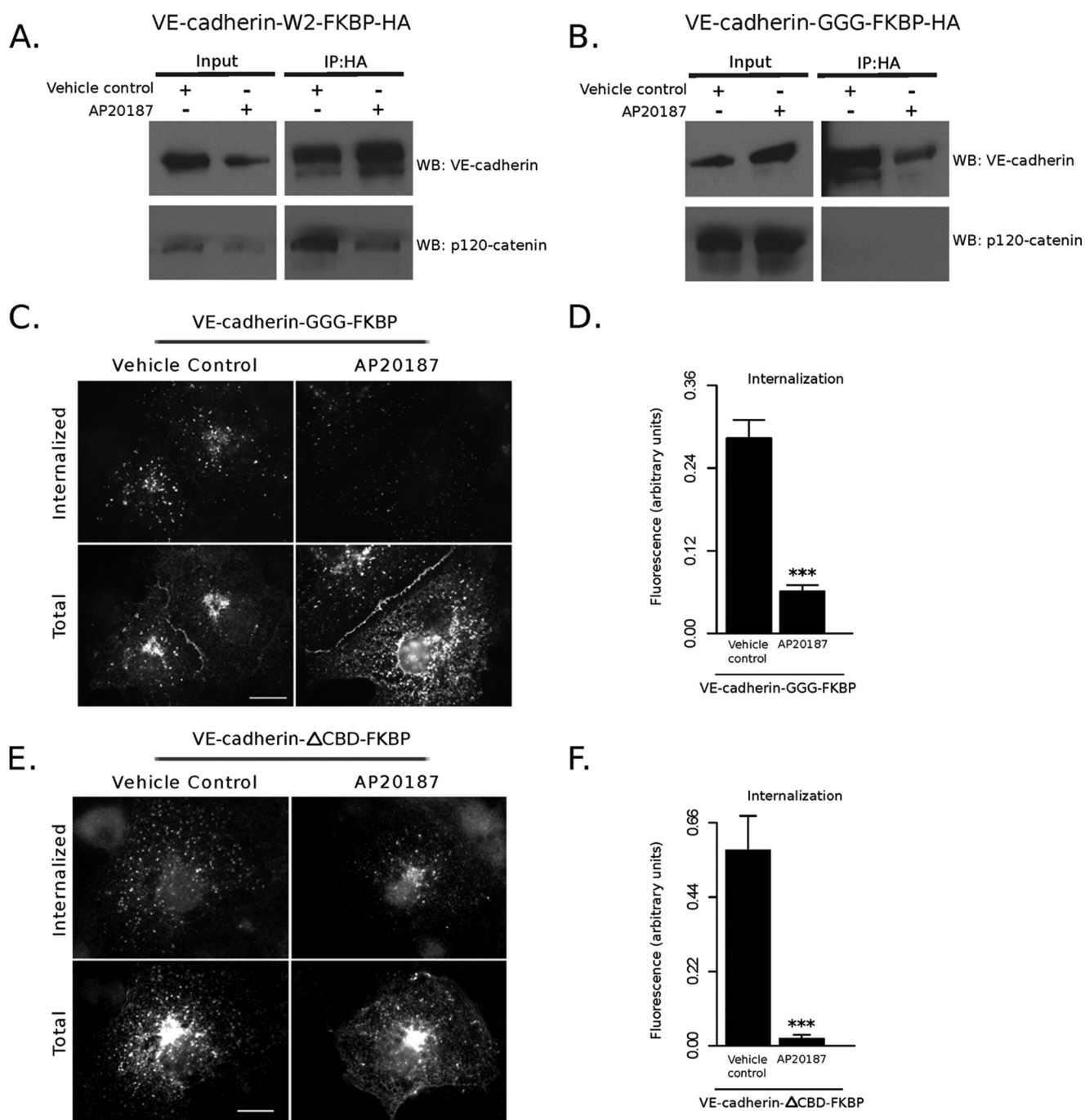


FIGURE 3. **p120-catenin binding is not required for inhibited dimer internalization.** *A* and *B*, isolation of VE-cadherin-Trp-2-FKBP (*A*) or VE-cadherin-GGG-FKBP (*B*) by immunoprecipitation (*IP*) using an antibody against the C terminus HA tag. Shown are Western blots (*WB*) for VE-cadherin (*top panels*) and p120 (*bottom panels*). *C* and *E*, fluorescence-based internalization assays of VE-cadherin-GGG-FKBP (*C*) or VE-cadherin-ΔCBD-FKBP (*E*) in COS-7 cells after treatment with vehicle control (*left panels*) or AP20187 (*right panels*). Scale bars = 20 μm. *D* and *F*, quantification of internalization. Error bars represent mean ± S.E. *n* > 20 cell/group. \*\*\*, *p* < 0.001.

estingly, we observed a decrease in colocalization between ankyrin-G and VE-cadherin-Trp-2 (Fig. 4, *D* and *E*).

To further investigate the association between ankyrin-G and VE-cadherin, we performed co-immunoprecipitation assays. We exogenously expressed the 190-kD isoform of HA-tagged ankyrin-G and VE-cadherin in COS-7 cells, which do not express endogenous VE-cadherin. Wild-type VE-cadherin co-immunoprecipitated with ankyrin-G (Fig. 4, *F* and *G*). Consistent with the colocalization results, we were unable to

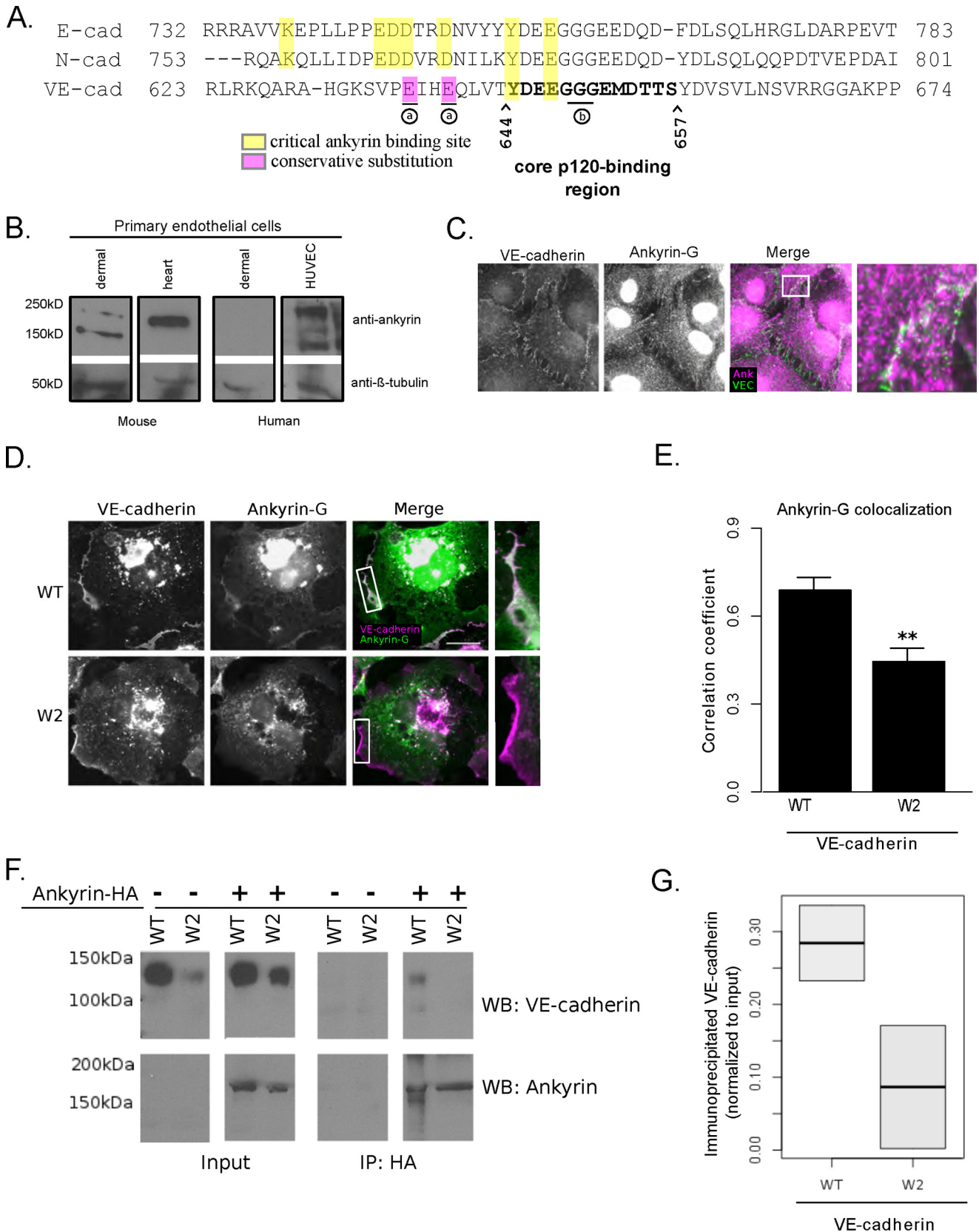
detect ankyrin-G association with VE-cadherin-Trp-2 (Fig. 4, *F* and *G*).

**Ankyrin-G Inhibits Internalization of VE-cadherin Independent of p120-catenin Binding**—Because ankyrin-G inhibits the endocytosis of E-cadherin localized to the lateral membrane of polarized epithelial cells, we reasoned that it might inhibit VE-cadherin endocytosis. To address this question, we performed internalization assays in cells exogenously expressing both VE-cadherin and ankyrin-G. Expression of ankyrin-G inhibited

## Ankyrin-G Inhibits Endocytosis of Cadherin Dimers

internalization of VE-cadherin (Fig. 5, A and B). Additionally, expression of ankyrin-G inhibited internalization of VE-cadherin-GGG (Fig. 5, C and D) and VE-cadherin- $\Delta$ CBD (Fig. 5, E

and F), which are unable to bind to p120 or  $\beta$ -catenin, respectively. However, ankyrin-G expression did not inhibit internalization of the transferrin receptor (Fig. 5, G and H). Therefore,



ankyrin-G does not inhibit endocytosis globally, but, instead, it selectively inhibits the endocytosis of VE-cadherin. These data suggest that ankyrin-G specifically inhibits the endocytosis of VE-cadherin independent of catenin binding.

**Ankyrin-G Selectively Associates with Dimerized VE-cadherin and Does Not Inhibit Endocytosis of the Trp-2 Mutant**—Our co-immunoprecipitation and colocalization results suggest that ankyrin-G binds to dimerized VE-cadherin. Because *cis* dimers may not form in the absence of *trans* interactions, we wanted to determine which type of VE-cadherin dimer, *cis* or *trans*, associates with ankyrin-G. To address this question, we induced *cis* dimerization of the VE-cadherin-Trp-2-FKBP mutant in cells exogenously expressing ankyrin-G. We observed that induced dimerization of the Trp-2 mutant resulted in ankyrin-G colocalization similar to wild-type VE-cadherin (Fig. 6, A and B). Therefore, we conclude that ankyrin-G selectively associates with *cis*-dimerized VE-cadherin.

Our colocalization results indicate that ankyrin-G associates with VE-cadherin upon *cis* dimerization of the cadherin. Therefore, we predicted that ankyrin-G would not inhibit endocytosis of the Trp-2 mutant. Consistent with this prediction, we found that VE-cadherin-Trp-2 internalization was not inhibited by ankyrin-G expression (Fig. 6, C and D). These data indicate that ankyrin-G-mediated inhibition of VE-cadherin internalization requires cadherin *cis* dimerization.

**Ankyrin-G Association Is Required to Inhibit VE-cadherin Dimer Internalization**—Our data suggest that ankyrin-G associates with and inhibits the internalization of *cis*-dimerized VE-cadherin. To directly test this idea, we mutated two glutamic acid residues, Glu-637 and Glu-640, to alanines. These amino acids represent acidic residues that are conserved in the ankyrin-G binding site in E-cadherin (Fig. 4A). To avoid complications from p120 binding to the dimers, we made the mutations in the VE-cadherin-GGG-FKBP mutant to create VE-cadherin-EE-GGG-FKBP. We observed a decrease in ankyrin-G colocalization with VE-cadherin-EE-GGG compared with VE-cadherin-GGG (Fig. 7, A and B). Additionally, we observed a significant increase in internalization of VE-cadherin-EE-GGG compared with wild-type VE-cadherin. Internalization of VE-cadherin-EEGGG was also increased compared with VE-cadherin-GGG, although the increase was not statistically significant (Fig. 7, C and D). Similar to the Trp-2 mutant, ankyrin-G expression did not inhibit internalization of the VE-cadherin-EE-GGG mutant (Fig. 7, E and F). Moreover, unlike the other VE-cadherin-FKBP fusion proteins, we found that inducing the dimerization of VE-cadherin-EE-GGG-FKBP did not result in a significant inhibition of internalization (Fig. 7, G and H). These

data indicate that ankyrin-G association is required to inhibit VE-cadherin dimer internalization.

**Ankyrin-G Regulates Adherens Junction Organization in Endothelial Cells**—Our data demonstrate that ankyrin-G inhibits endocytosis of VE-cadherin dimers in COS-7 cells and localizes with VE-cadherin at endothelial cell junctions. Therefore, we reasoned that ankyrin-G may play a role in stabilizing VE-cadherin at the cell surface of endothelial cells. To test this hypothesis, we transfected HUVECs with shRNA against ankyrin-G. We observed a significant decrease in ankyrin-G signal in HUVECs transfected with ankyrin-G shRNA compared with cells transfected with control shRNA by immunofluorescence microscopy (Fig. 8A). Additionally, a Western blot of cell lysate from HUVECs transfected with control shRNA against luciferase or shRNA against ankyrin-G confirmed a decrease in the 190-kD isoform of ankyrin-G (Fig. 8B). We observed a significant decrease in adherens junction proteins, including VE-cadherin, p120-catenin, and  $\beta$ -catenin, at junctions after ankyrin-G knockdown compared with control knockdown (Fig. 8A). Importantly, co-transfection of ankyrin shRNA with an HA-tagged 190-kD ankyrin-G that is refractory to the shRNA (Fig. 8B, right panel) resulted in levels of junctional VE-cadherin similar to the control (Fig. 8C). Moreover, we found that knockdown of ankyrin-G increased the internalization of wild-type VE-cadherin, although it did not reach statistical significance. This outcome is likely due to p120 binding to the cadherin and masking the effects of ankyrin knockdown (Fig. 8D). Therefore, to assess the effect of ankyrin-G knockdown in the absence of p120 binding, we performed an internalization assay of VE-cadherin-GGG in cells transfected with ankyrin-G shRNA and found a significant increase in internalization compared with cells transfected with control shRNA (Fig. 8E). Together, these data suggest that ankyrin-G inhibits the endocytosis of VE-cadherin in endothelial cells and regulates the organization of endothelial adherens junctions.

## Discussion

Membrane trafficking has emerged as a major mechanism that regulates cadherin adhesion. However, the mechanisms that control VE-cadherin endocytosis are not fully understood. The results presented here demonstrate that *cis* dimerization of VE-cadherin inhibits endocytosis. Furthermore, inhibition of endocytosis occurs in a manner independent of adhesive interactions (*trans* dimerization) (Fig. 2, C and D) and independent of p120 binding (Fig. 3). The mechanism by which *cis* dimerization inhibits endocytosis was also investigated. Our data reveal that ankyrin-G stabilizes the cadherin at the cell surface (Fig. 5, A and B). This process requires cadherin *cis* dimerization but

**FIGURE 4. Ankyrin-G associates with the juxtamembrane domain of VE-cadherin.** A, sequence alignment of the juxtamembranes of classical cadherins. Critical ankyrin-G binding sites are highlighted in yellow. Conservative substitutions are highlighted in pink. The core p120-binding region is identified by boldface print. a, VE-cadherin mutations used in Fig. 7. b, VE-cadherin mutations used in Figs. 3, 5, and 7. B, Western blot for ankyrin-G (top) and  $\beta$ -tubulin (bottom) as a loading control. Samples from left to right show primary mouse dermal endothelial cells or heart endothelial cells and primary human dermal microvascular endothelial cells or HUVECs. Note that only the 210-kD ankyrin-G isoform is detectable in mouse heart endothelial cells. C, immunofluorescence of VE-cadherin (VEC) and ankyrin-G (Ank) in HUVECs. The area in the white box is enlarged in the fourth panel. D, colocalization of ankyrin-G with the wild type (top panels) or the Trp-2 (bottom panels) cadherin mutant. The areas in the white rectangles are enlarged in the fourth panels. An intense perinuclear signal was excluded from the analysis. Scale bar = 20  $\mu$ m. E, quantification of the colocalization in B. y Axis, Pearson's correlation coefficient.  $n > 20$  cells/group \*\*,  $p < 0.01$ . F, co-immunoprecipitation (IP) of cell lysates exogenously expressing either VE-cadherin or both ankyrin-G-HA and VE-cadherin. An anti-HA antibody was used to isolate ankyrin-G-HA, and Western blot analyses for VE-cadherin (top panels) and ankyrin-G (bottom panels) were performed. Cadherin proteins: WT or non-adhesive (Trp-2). G, densitometric quantification of the Western blot in D ( $n = 2$ ).

## Ankyrin-G Inhibits Endocytosis of Cadherin Dimers

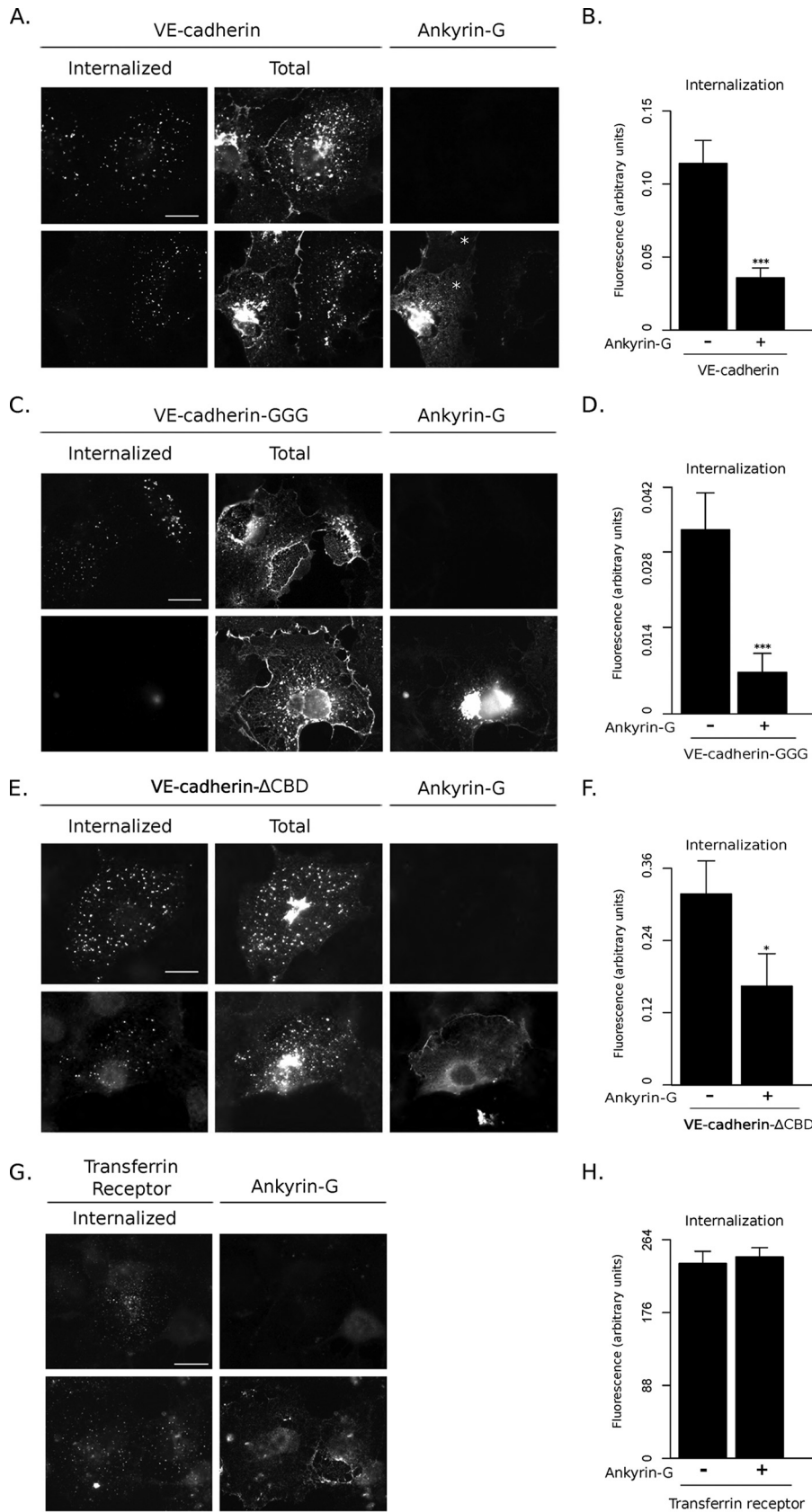


**FIGURE 5. Ankyrin-G inhibits internalization of VE-cadherin.** Endocytosis of wild-type VE-cadherin (A and B), VE-cadherin-GGG (C and D), VE-cadherin-ΔCBD (E and F), or the transferrin receptor (G and H) without (A, C, E, and G, top panels) or with (A, C, E, and G, bottom panels) exogenous ankyrin-G expression was measured with a fluorescence-based internalization assay. A, asterisks mark cells in the view expressing both VE-cadherin and ankyrin-G. B and D, error bars represent mean  $\pm$  S.E.  $n = 20$  cells/group. \*\*\*,  $p < 0.001$ . F, error bars represent mean S.E.  $n = 10$  cells/group. \*,  $p < 0.05$ . H, error bars represent mean S.E.  $n > 20$  cells/group. Scale bars = 20  $\mu$ m.

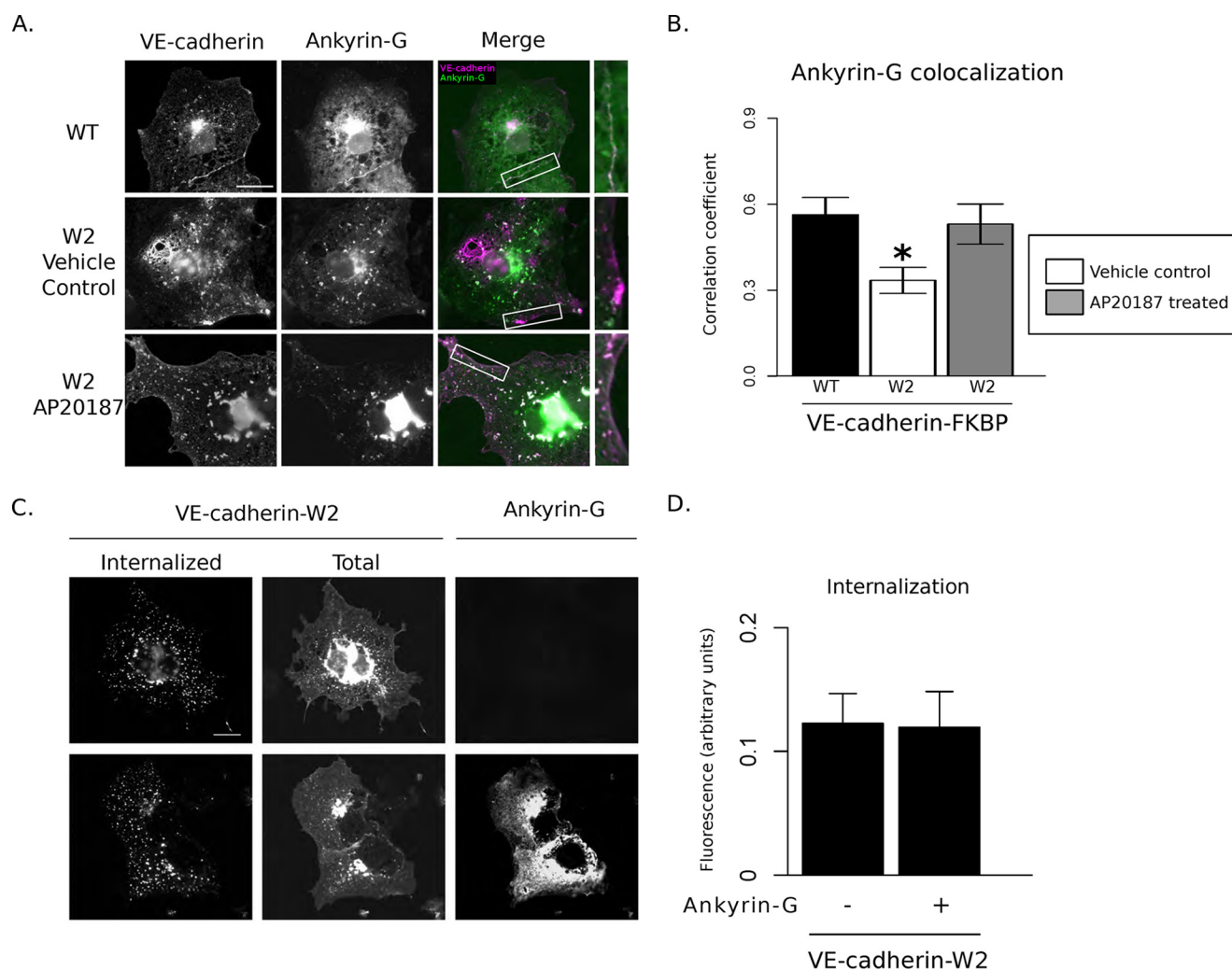


**FIGURE 6. Ankyrin-G associates with VE-cadherin dimers and does not inhibit endocytosis of the Trp-2 mutant.** *A*, colocalization of ankyrin-G with wild-type VE-cadherin (*top panels*), the vehicle control-treated Trp-2 mutant (*center panels*), or the AP20187-treated Trp-2 mutant (*bottom panels*). The areas in the *white rectangles* are enlarged in the *fourth panels*. An intense perinuclear signal was excluded from the analysis. *B*, quantification of colocalization. *y Axis*, Pearson's correlation coefficient. *Error bars* represent mean  $\pm$  S.E.  $n = 8$  cells/group.  $*$ ,  $p < 0.05$  compared with the WT. *C*, internalization assay of VE-cadherin-W2 without (*top panels*) and with (*bottom panels*) exogenous ankyrin-G expression. *D*, quantification of internalization. *Error bars* represent mean  $\pm$  S.E.  $n > 15$  cells/group. *Scale bars* = 20  $\mu$ m.

not p120 binding nor cadherin linkage to the actin cytoskeleton through association with  $\beta$ -catenin. Collectively, our results support a model in which ankyrin-G associates with and inhibits the internalization of VE-cadherin *cis* dimers (Fig. 9).

The role of adhesion in the regulation of cadherin endocytosis is not fully understood. Interestingly, dimerization of other cell surface receptors, including receptor tyrosine kinases and G protein-coupled receptors, results in increased endocytosis from the plasma membrane (30, 31). The results presented here suggest a distinct mechanism of regulation for cadherin endocytosis. We find that mutating a tryptophan residue critical for adhesion results in increased cadherin endocytosis. However, increased endocytosis appears to result from a loss of cadherin *cis* dimers rather than from a loss of adhesion. This conclusion is made on the basis of the finding that forcing *cis* dimerization of a cadherin mutant unable to engage in adhesion virtually abolished VE-cadherin endocytosis. Additionally, p120 binding to the cadherin tail is not required for *cis* dimerization to inhibit endocytosis (Fig. 3, *B–D*). This result was surprising because

p120 is widely known to be a key regulator of cadherin stability at the plasma membrane.

Here we report that ankyrin-G associates with VE-cadherin and inhibits its endocytosis (Figs. 4 and 5). Ankyrin-G binding partners are known to include other cell adhesion molecules, including L1 cell adhesion molecule and E- and N-cadherin. The ankyrin-G binding sites in these proteins are stretches of 10–20 amino acids that do not contain a single defining motif (22). Instead, the ankyrin-G binding site is different between families of proteins. However, it is typically conserved within a family of proteins. For example, the ankyrin-G-binding site in E- and N-cadherin consists of a stretch of 21 amino acids with seven conserved amino acids that are critical for binding. This ankyrin-G-binding motif is not fully conserved in VE-cadherin (Fig. 4A). Despite these differences in this region of the VE-cadherin tail, our data demonstrate that ankyrin-G associates with the cytoplasmic tail of VE-cadherin. First, we observe colocalization of ankyrin-G and VE-cadherin in primary endothelial cells and when expressed exogenously in other cell types

## Ankyrin-G Inhibits Endocytosis of Cadherin Dimers

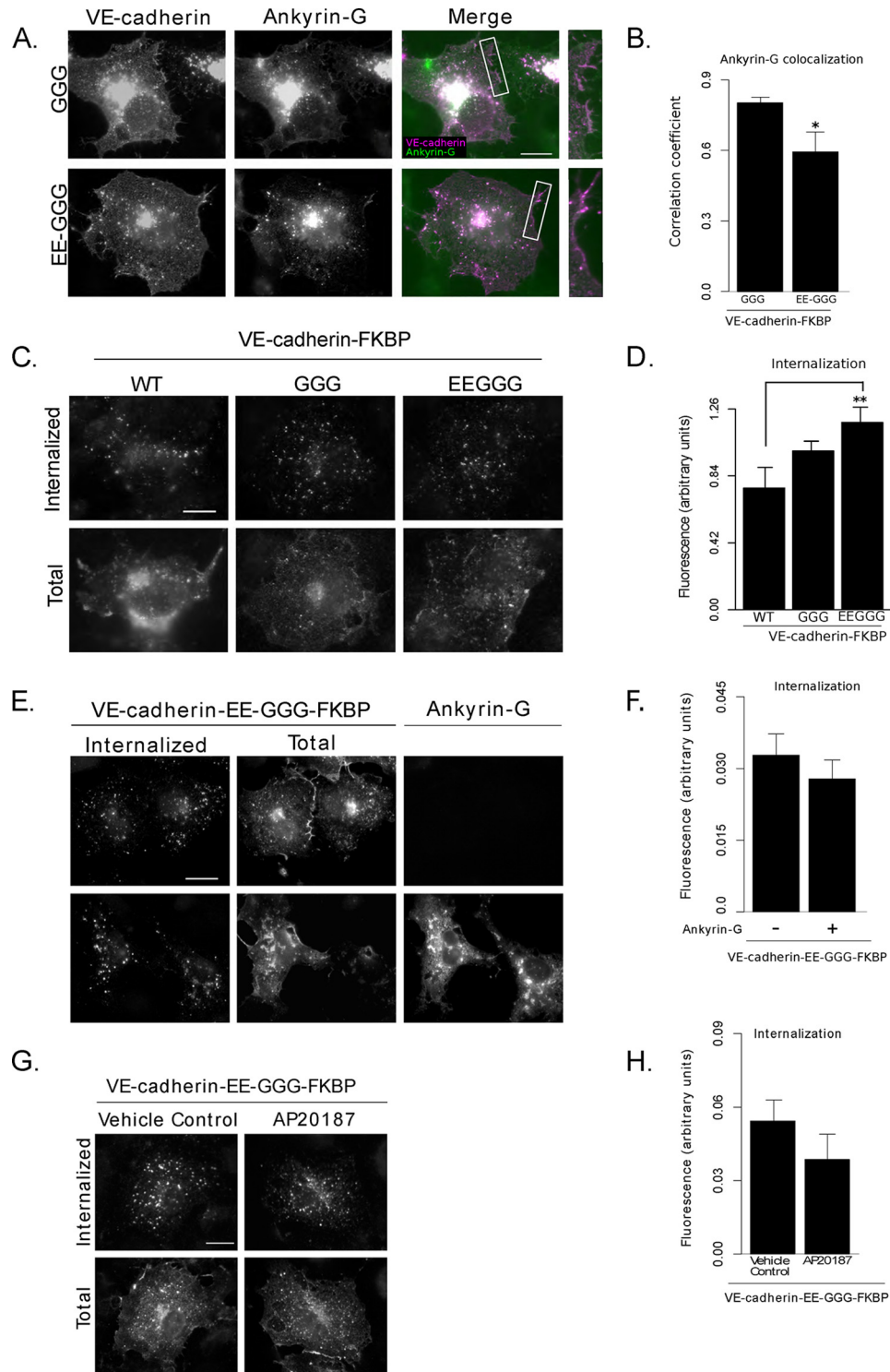
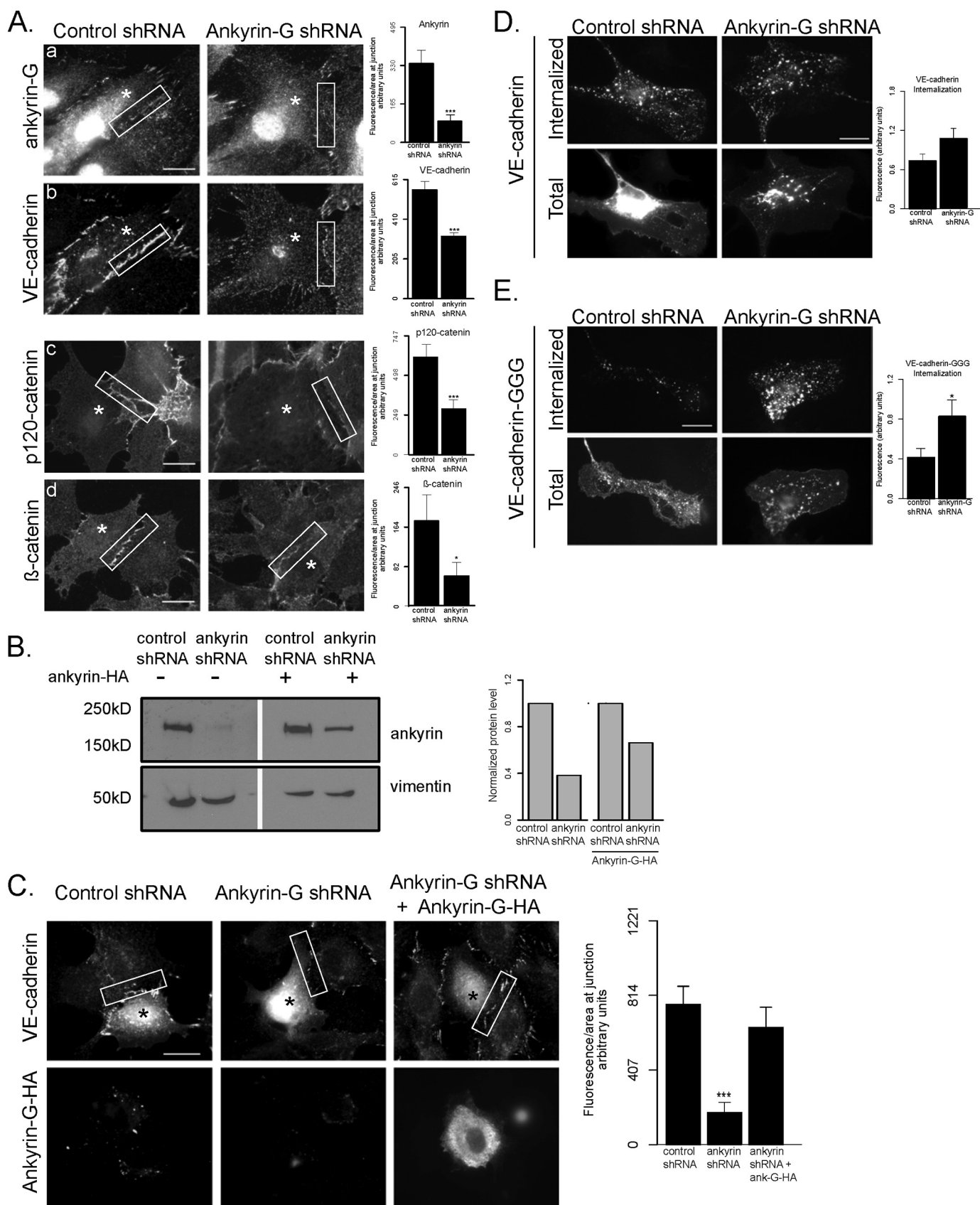


**FIGURE 7. Ankyrin-G association is required to inhibit VE-cadherin dimer internalization.** *A*, colocalization of ankyrin-G with the VE-cadherin-GGG mutant (top panels) or the VE-cadherin-EE-GGG mutant (bottom panels). The areas in the white rectangles are enlarged in the left panels. An intense perinuclear signal was excluded from the analysis. Scale bar = 20  $\mu\text{m}$ . *B*, quantification of colocalization. *y* Axis, Pearson's correlation coefficient. Error bars represent mean  $\pm$  S.E.  $n > 20$  cells/group. \*,  $p < 0.05$  compared with VE-cadherin-GGG. *C*, internalization assay of VE-cadherin-EE-GGG-FKBP compared with VE-cadherin-WT and VE-cadherin-GGG in COS-7 cells. Scale bar = 20  $\mu\text{m}$ . *D*, quantification of the internalization shown in *C*. Error bars represent mean  $\pm$  S.E.  $n > 15$  cells. \*\*,  $p < 0.01$  compared with VE-cadherin-WT. *E*, endocytosis of VE-cadherin-EE-GGG without (top panels) and with (bottom panels) exogenous ankyrin-G expression measured with a fluorescence-based internalization assay. Scale bar = 20  $\mu\text{m}$ . *F*, quantification of internalization. Error bars represent mean  $\pm$  S.E.  $n > 20$  cells/group. *G*, fluorescence-based internalization assay of VE-cadherin-EE-GGG-FKBP after treatment with vehicle control (left panels) or AP20187 (right panels). Scale bar = 20  $\mu\text{m}$ . *H*, quantification of internalization. Error bars represent mean  $\pm$  S.E.  $n > 25$  cell/group.

(Fig. 4, *C–E*). In addition, we found that wild-type VE-cadherin co-immunoprecipitates with ankyrin-G. Importantly, the VE-cadherin-Trp-2 mutant, which is unable to engage in adhesion,

does not co-immunoprecipitate with ankyrin-G, indicating that ankyrin-G association is specific and requires dimerization (either *cis* or *trans*) of the cadherin.



## Ankyrin-G Inhibits Endocytosis of Cadherin Dimers

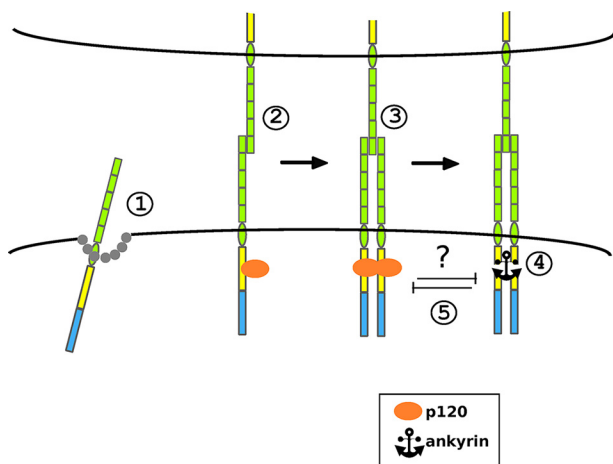


**FIGURE 9. Model of ankyrin-G-mediated inhibition of the internalization of VE-cadherin dimers.** 1, VE-cadherin monomers are internalized when not bound by p120. 2, p120 stabilizes cadherin at the plasma membrane, and *trans* interactions form between two VE-cadherin proteins on neighboring cells. 3, after the formation of *cis* interactions, p120 (3) or ankyrin-G (4) bind to and stabilize VE-cadherin. 5, whether p120 and ankyrin-G bind to VE-cadherin simultaneously is not known.

The data presented here as well as work published previously by Jenkins *et al.* establish ankyrin-G as a novel regulator of cadherin endocytosis (24). Furthermore, ankyrin-G and p120-catenin inhibit cadherin internalization in mechanistically distinct ways. For example, p120 associates with and potently inhibits endocytosis of cadherins that are unable to engage in adhesion, including IL2-VE-cadherin chimeras that lack the entire cadherin extracellular domain (9). In contrast, ankyrin-G selectively associates with dimerized cadherin (Fig. 4) and does not associate with or prevent endocytosis of VE-cadherin mutants that are unable to form dimers. This finding is consistent with reports that ankyrin-G binds to specific receptors, such as neurofascin, only when dimerized (34). The precise mechanisms by which ankyrin-G regulates internalization is not fully understood, but it does not appear to require linkage to the actin cytoskeleton through  $\beta$ -catenin because ankyrin-G inhibited the internalization of a VE-cadherin mutant lacking the catenin-binding domain. Because VE-cadherin shares only a portion of the conserved ankyrin-G-binding motif, it is possible that dimerization provides a platform capable of stabilizing the VE-cadherin-ankyrin-G interaction.

The VE-cadherin juxtamembrane domain in the cytoplasmic tail contains a dual function motif that serves as either a p120-binding site or as an endocytic motif (6). When p120 is bound to this motif, clathrin-dependent endocytosis of the cadherin is potently inhibited. Because ankyrin-G binds to the juxtamem-

brane domain of classic cadherins (23), it is possible that ankyrin-G inhibits VE-cadherin endocytosis in a similar manner. However, we cannot rule out that ankyrin-G may regulate VE-cadherin endocytosis indirectly through association with other proteins reported to modulate cadherin endocytosis, such as Numb. However, this seems unlikely because Numb associates with p120-catenin to regulate endocytosis of E-cadherin (35), and we found that ankyrin-G inhibits endocytosis of the VE-cadherin-GGG mutant, which does not bind to p120 (Fig. 3B). Therefore, we favor a model in which ankyrin-G interacts with VE-cadherin directly to modulate endocytosis (Fig. 9).

It remains to be determined whether the binding of p120 and ankyrin-G to the cadherin is mutually exclusive. However, given the mass of both p120 and ankyrin-G and the location of critical ankyrin-G residues in the core p120-binding region, it is unlikely that both proteins bind to the cadherin simultaneously. Therefore, it is highly likely that different subcellular pools of cadherin are stabilized by either p120 or ankyrin-G and that these binding partners differentially regulate cadherin stability at the plasma membrane. For example, it is possible that ankyrin-G and p120 inhibit the endocytosis of different pools of VE-cadherin at different membrane domains, such as at junctional or non-junctional regions of the plasma membrane. Consistent with this possibility, a recent study has found that ankyrin-G is concentrated in microdomains in the lateral membrane of Madin-Darby canine kidney cells (38). Furthermore, the giant ankyrin-G isoform stabilizes GABAergic synapses by opposing endocytosis in microdomains in the somatodendritic plasma membrane of hippocampal neurons (36, 37). Moreover, a recent report from Jenkins *et al.* reports micron-sized domains consisting of an underlying membrane skeleton comprised of ankyrin-G and its partner  $\beta$ -spectrin that inhibit endocytosis through the exclusion of clathrin and clathrin-dependent cargo in epithelial lateral membranes (38). It is possible that ankyrin-G, in conjunction with  $\beta$ -spectrin, inhibits VE-cadherin endocytosis through clathrin exclusion at microdomains in endothelial cells (38).

Our data suggest that ankyrin-G regulates adherens junction organization because knockdown of the protein results in significantly less cadherin, p120-catenin, and  $\beta$ -catenin at junctions (Fig. 8A). These observations suggest a key role for ankyrin-G in the regulation of endothelial functions that rely on adherens junctions, such as signaling and barrier functions (2, 39, 40). The identification of ankyrin, in addition to p120, as a modulator of cadherin trafficking suggests that the cadherin juxtamembrane domain may interact with a number of different proteins in different cellular contexts to regulate cadherin

**FIGURE 8. Ankyrin-G regulates adherens junction organization in endothelial cells.** *A, left panel*, immunofluorescence of HUVECs after transfection with luciferase shRNA (control) or ankyrin-G shRNA. Shown is the immunofluorescence of ankyrin-G (a), VE-cadherin (b), p120-catenin (c), and  $\beta$ -catenin (d) after transfection with luciferase shRNA or ankyrin-G shRNA. *Right panel*, quantification. Asterisks mark transfected cells determined by mCherry expression. Rectangles highlight junctions. Scale bar = 20  $\mu$ m. Error bars represent mean  $\pm$  S.E.  $n > 15$  junctions/groups. \*\*\*,  $p < 0.001$ ; \*,  $p < 0.05$ . *B, left panel*, Western blot of whole cell lysates from HUVECs after transfection with luciferase shRNA (control) or ankyrin-G shRNA. *Top*, ankyrin-G. *Bottom*, vimentin loading control. *Left*, shRNA only. *Right*, shRNA plus HA-tagged 190-kD ankyrin-G. *Right panel*, quantification of protein levels normalized to luciferase shRNA control or luciferase shRNA plus HA-tagged 190-kD ankyrin-G. *C, left panel*, immunofluorescence of HUVECs expressing control shRNA, ankyrin-G shRNA, or ankyrin-G shRNA plus HA-tagged 190-kD ankyrin-G. *Top row*, VE-cadherin. *Bottom row*, ankyrin-G-HA. The rectangles highlight cell junctions. Asterisks mark transfected cells determined by mCherry expression. *Right panel*, quantification of VE-cadherin at junctions. Scale bar = 20  $\mu$ m. Error bars represent mean  $\pm$  S.E.  $n > 25$  junctions/groups. \*\*\*,  $p < 0.001$ . *D*, internalization of exogenously expressed VE-cadherin (wild-type) in HUVECs in cells transfected with luciferase shRNA or ankyrin-G shRNA. Scale bar = 20  $\mu$ m. Error bars represent mean  $\pm$  S.E.  $n > 25$  cell/group. *E*, internalization of exogenously expressed VE-cadherin-GGG in HUVECs in cells transfected with luciferase shRNA or ankyrin-G shRNA. Scale bar = 20  $\mu$ m. Error bars represent mean  $\pm$  S.E.  $n > 30$  cells/group. \*,  $p < 0.05$ .

levels at the plasma membrane. It is likely that additional binding partners for this cadherin domain will emerge as regulators of cadherin endocytosis. Further studies are needed to gain insights into the specific role of p120 and ankyrin-G in regulating cadherin internalization to modulate cell adhesion in various developmental and disease contexts.

**Author Contributions**—A. P. K. and C. M. C. conceived and coordinated the study and wrote the paper. C. M. C. designed, performed, and analyzed the experiments. C. M. C. and P. M. J. designed and constructed vectors for the expression of mutant proteins. P. M. J. and V. B. provided technical input as well as intellectual contributions to the drafting of the manuscript and figures. All authors reviewed the results and approved the final version of the manuscript.

**Acknowledgments**—We thank Dr. Benjamin Nanes for customizing ImageJ plugins for the automation of data quantification. We also thank Susan Summers for help with virus propagation and cell culture and Oskar Laur at the Emory Custom Cloning Core Facility for generation of the  $\Delta$ CBD and EE-GGG VE-cadherin-FKBP plasmids.

## References

- Carmeliet, P. (2003) Angiogenesis in health and disease. *Nat. Med.* **9**, 653–660
- Dejana, E., Orsenigo, F., and Lampugnani, M. G. (2008) The role of adherens junctions and VE-cadherin in the control of vascular permeability. *J. Cell Sci.* **121**, 2115–2122
- Vincent, P. A., Xiao, K., Buckley, K. M., and Kowalczyk, A. P. (2004) VE-cadherin: adhesion at arm's length. *Am. J. Physiol. Cell Physiol.* **286**, C987–997
- Saito, M., Tucker, D. K., Kohlhorst, D., Niessen, C. M., and Kowalczyk, A. P. (2012) Classical and desmosomal cadherins at a glance. *J. Cell Sci.* **125**, 2547–2552
- Harris, E. S., and Nelson, W. J. (2010) VE-cadherin: at the front, center, and sides of endothelial cell organization and function. *Curr Opin Cell Biol.* **22**, 651–658
- Nanes, B. A., Chiasson-MacKenzie, C., Lowery, A. M., Ishiyama, N., Faundez, V., Ikura, M., Vincent, P. A., and Kowalczyk, A. P. (2012) p120-catenin binding masks an endocytic signal conserved in classical cadherins. *J. Cell Biol.* **199**, 365–380
- Chiasson, C. M., Wittich, K. B., Vincent, P. A., Faundez, V., and Kowalczyk, A. P. (2009) p120-catenin inhibits VE-cadherin internalization through a Rho-independent mechanism. *Mol. Biol. Cell* **20**, 1970–1980
- Davis, M. A., Ireton, R. C., and Reynolds, A. B. (2003) A core function for p120-catenin in cadherin turnover. *J. Cell Biol.* **163**, 525–534
- Xiao, K., Allison, D. F., Buckley, K. M., Kottke, M. D., Vincent, P. A., Faundez, V., and Kowalczyk, A. P. (2003) Cellular levels of p120 catenin function as a set point for cadherin expression levels in microvascular endothelial cells. *J. Cell Biol.* **163**, 535–545
- Xiao, K., Allison, D. F., Kottke, M. D., Summers, S., Sorescu, G. P., Faundez, V., and Kowalczyk, A. P. (2003) Mechanisms of VE-cadherin processing and degradation in microvascular endothelial cells. *J. Biol. Chem.* **278**, 19199–19208
- Desai, R., Sarpal, R., Ishiyama, N., Pellikka, M., Ikura, M., and Tepass, U. (2013) Monomeric  $\alpha$ -catenin links cadherin to the actin cytoskeleton. *Nat. Cell Biol.* **15**, 261–273
- Taguchi, K., Ishiuchi, T., and Takeichi, M. (2011) Mechanosensitive EPLIN-dependent remodeling of adherens junctions regulates epithelial reshaping. *J. Cell Biol.* **194**, 643–656
- Yamada, S., Pokutta, S., Drees, F., Weis, W. I., and Nelson, W. J. (2005) Deconstructing the cadherin-catenin-actin complex. *Cell* **123**, 889–901
- Oas, R. G., Nanes, B. A., Esimai, C. C., Vincent, P. A., García, A. J., and Kowalczyk, A. P. (2013) p120-catenin and  $\beta$ -catenin differentially regulate cadherin adhesive function. *Mol. Biol. Cell* **24**, 704–714
- Pokutta, S., Drees, F., Yamada, S., Nelson, W. J., and Weis, W. I. (2008) Biochemical and structural analysis of  $\alpha$ -catenin in cell-cell contacts. *Biochem. Soc. Trans.* **36**, 141–147
- Brasch, J., Harrison, O. J., Honig, B., and Shapiro, L. (2012) Thinking outside the cell: how cadherins drive adhesion. *Trends Cell Biol.* **22**, 299–310
- Zhang, Y., Sivasankar, S., Nelson, W. J., and Chu, S. (2009) Resolving cadherin interactions and binding cooperativity at the single-molecule level. *Proc. Natl. Acad. Sci. U.S.A.* **106**, 109–114
- Shapiro, L., Fannon, A. M., Kwong, P. D., Thompson, A., Lehmann, M. S., Grubel, G., Legrand, J. F., Als-Nielsen, J., Colman, D. R., and Hendrickson, W. A. (1995) Structural basis of cell-cell adhesion by cadherins. *Nature* **374**, 327–337
- Brasch, J., Harrison, O. J., Ahlsen, G., Carnally, S. M., Henderson, R. M., Honig, B., and Shapiro, L. (2011) Structure and binding mechanism of vascular endothelial cadherin: a divergent classical cadherin. *J. Mol. Biol.* **408**, 57–73
- Harrison, O. J., Jin, X., Hong, S., Bahna, F., Ahlsen, G., Brasch, J., Wu, Y., Vendome, J., Felsovalyi, K., Hampton, C. M., Troyanovsky, R. B., Ben-Shaul, A., Frank, J., Troyanovsky, S. M., Shapiro, L., and Honig, B. (2011) The extracellular architecture of adherens junctions revealed by crystal structures of type I cadherins. *Structure* **19**, 244–256
- Prasain, N., and Stevens, T. (2009) The actin cytoskeleton in endothelial cell phenotypes. *Microvasc. Res.* **77**, 53–63
- Bennett, V., and Healy, J. (2009) Membrane domains based on ankyrin and spectrin associated with cell-cell interactions. *Cold Spring Harb. Perspect. Biol.* **1**, a003012
- Kizhatil, K., Davis, J. Q., Davis, L., Hoffman, J., Hogan, B. L., and Bennett, V. (2007) Ankyrin-G is a molecular partner of E-cadherin in epithelial cells and early embryos. *J. Biol. Chem.* **282**, 26552–26561
- Jenkins, P. M., Vasavda, C., Hostettler, J., Davis, J. Q., Abdi, K., and Bennett, V. (2013) E-cadherin polarity is determined by a multifunction motif mediating lateral membrane retention through ankyrin-G and apical-lateral transcytosis through clathrin. *J. Biol. Chem.* **288**, 14018–14031
- Oas, R. G., Xiao, K., Summers, S., Wittich, K. B., Chiasson, C. M., Martin, W. D., Grossniklaus, H. E., Vincent, P. A., Reynolds, A. B., and Kowalczyk, A. P. (2010) p120-Catenin is required for mouse vascular development. *Circ. Res.* **106**, 941–951
- Kizhatil, K., and Bennett, V. (2004) Lateral membrane biogenesis in human bronchial epithelial cells requires 190-kDa ankyrin-G. *J. Biol. Chem.* **279**, 16706–16714
- Schneider, C. A., Rasband, W. S., and Eliceiri, K. W. (2012) NIH Image to ImageJ: 25 years of image analysis. *Nat. Methods* **9**, 671–675
- May, C., Doody, J. F., Abdullah, R., Balderes, P., Xu, X., Chen, C. P., Zhu, Z., Shapiro, L., Kussie, P., Hicklin, D. J., Liao, F., and Bohlen, P. (2005) Identification of a transiently exposed VE-cadherin epitope that allows for specific targeting of an antibody to the tumor neovasculature. *Blood* **105**, 4337–4344
- Broermann, A., Winderlich, M., Block, H., Frye, M., Rossaint, J., Zarbock, A., Cagna, G., Linnepe, R., Schulte, D., Nottebaum, A. F., and Vestweber, D. (2011) Dissociation of VE-PTP from VE-cadherin is required for leukocyte extravasation and for VEGF-induced vascular permeability *in vivo*. *J. Exp. Med.* **208**, 2393–2401
- Hofman, E. G., Bader, A. N., Voortman, J., van den Heuvel, D. J., Sigismund, S., Verkleij, A. J., Gerritsen, H. C., and van Bergen en Henegouwen, P. M. (2010) Ligand-induced EGF receptor oligomerization is kinase-dependent and enhances internalization. *J. Biol. Chem.* **285**, 39481–39489
- Song, G. J., and Hinkle, P. M. (2005) Regulated dimerization of the thyrotropin-releasing hormone receptor affects receptor trafficking but not signaling. *Mol. Endocrinol.* **19**, 2859–2870
- Chen, J., Nekrasova, O. E., Patel, D. M., Klessner, J. L., Godsel, L. M., Koetsier, J. L., Amargo, E. V., Desai, B. V., and Green, K. J. (2012) The C-terminal unique region of desmoglein 2 inhibits its internalization via tail-tail interactions. *J. Cell Biol.* **199**, 699–711
- Yap, A. S., Briehner, W. M., Pruschy, M., and Gumbiner, B. M. (1997) Lateral clustering of the adhesive ectodomain: a fundamental determinant of cadherin function. *Curr. Biol.* **7**, 308–315

## Ankyrin-G Inhibits Endocytosis of Cadherin Dimers

34. Jefford, G., and Dubreuil, R. R. (2000) Receptor clustering drives polarized assembly of ankyrin. *J. Biol. Chem.* **275**, 27726–27732
35. Sato, K., Watanabe, T., Wang, S., Kakeno, M., Matsuzawa, K., Matsui, T., Yokoi, K., Murase, K., Sugiyama, I., Ozawa, M., and Kaibuchi, K. (2011) Numb controls E-cadherin endocytosis through p120 catenin with aPKC. *Mol. Biol. Cell* **22**, 3103–3119
36. He, M., Abdi, K. M., and Bennett, V. (2014) Ankyrin-G palmitoylation and  $\beta$ II-spectrin binding to phosphoinositide lipids drive lateral membrane assembly. *J. Cell Biol.* **206**, 273–288
37. Tseng, W. C., Jenkins, P. M., Tanaka, M., Mooney, R., and Bennett, V. (2015) Giant ankyrin-G stabilizes somatodendritic GABAergic synapses through opposing endocytosis of GABA<sub>A</sub> receptors. *Proc. Natl. Acad. Sci. U.S.A.* **112**, 1214–1219
38. Jenkins, P., Meng, H., Bennett, V. (2015) Dynamic spectrin/ankyrin-G microdomains promote lateral membrane assembly by opposing endocytosis. *Sci. Adv.* **1**, e1500301
39. Giannotta, M., Trani, M., and Dejana, E. (2013) VE-cadherin and endothelial adherens junctions: active guardians of vascular integrity. *Dev. Cell* **26**, 441–454
40. Hordijk, P. L., Anthony, E., Mul, F. P., Rientsma, R., Oomen, L. C., and Roos, D. (1999) Vascular-endothelial-cadherin modulates endothelial monolayer permeability. *J. Cell Sci.* **112**, 1915–1923

## **Ankyrin-G Inhibits Endocytosis of Cadherin Dimers**

Chantel M. Cadwell, Paul M. Jenkins, Vann Bennett and Andrew P. Kowalczyk

*J. Biol. Chem.* 2016, 291:691-704.

doi: 10.1074/jbc.M115.648386 originally published online November 16, 2015

---

Access the most updated version of this article at doi: [10.1074/jbc.M115.648386](https://doi.org/10.1074/jbc.M115.648386)

Alerts:

- [When this article is cited](#)
- [When a correction for this article is posted](#)

[Click here](#) to choose from all of JBC's e-mail alerts

This article cites 40 references, 27 of which can be accessed free at <http://www.jbc.org/content/291/2/691.full.html#ref-list-1>